Zagazig University Medical Journal
www.zumj.journals.ekb.eg
https://doi.org/10.21608/zumj.2024.279448.3283 Volume 30, Issue 4, July 2024
Manuscript ID ZUMJ-2403-3283 (R1)
DOI 10.21608/ZUMJ.2024.279448.3283
Original article

Assessment of the Therapeutic Impact of Ivermectin Loaded on Solid Lipid Nanoparticles against Muscular Phase of Murine Trichinosis

Tahani Ismail Farag*[1], Mona Hussein Almotayam[1], Asmaa Salah Nasr Mohamed[2], Al-Sayed R. Al-Attar[3], Ibrahim Aly[4], Shaimaa Mohamed Farag[1], Samar Kamel Hammad[1]
[1]Medical Parasitology department, Zagazig faculty of medicine, Zagazig, Egypt
[2]Medical Parasitology department, Fakous faculty of medicine, Fakous, Egypt
[3]Pathology department, Faculty of Veterinary Medicine, Zagazig University, Zagazig, Egypt
[4]Immunoparasitology Department, Theodor Bilharz Research Institute, Giza, Egypt

***Corresponding author:**
Tahani Ismail Farag

Email:
tahaniabdelkhalik2015@gmail.com

Submit Date 2024-03-30
Revise Date 2024-04-20
Accept Date 2024-04-25

Background: Trichinosis is acquired through ingesting the infective larvae in pork meat. Drugs employed for the treatment of trichinosis have a limited bioavailability in addition to the adverse side effects. In the current work, the therapeutic effect of ivermectin against experimental muscle trichinosis was evaluated using solid lipid nanoparticles with and without albendazole.
Methods: Seven groups of ten albino mice each were created from the 70 total. (GI): normal control, (GII): infected, non-treated, and (GIII): infected treated with albendazole, (GIV): infected treated with ivermectin. (GV) infected treated with solid lipid nanoparticles, (GVI): infected treated with ivermectin loaded on solid lipid nanoparticles, and (GVII): infected and received a combination of albendazole and solid lipid nanoparticles loaded with ivermectin. For the seven-day intestinal phase and the 49-day muscle phase, each group was split into two subgroups of five mice each. The focus of this study is the muscular phase. The mean number of encysted larvae in the muscle tissue was counted for a parasitological evaluation. Using feulgen and hematoxylin and eosin (H&E) stains, all groups were assessed histopathologically and histochemically, respectively. Liver and kidney parameters were also assessed biochemically.
Results: The treatment that combined the use of albendazole and ivermectin loaded on solid lipid nanoparticles (GVII) produced the greatest decrease in the count of encysted muscle larvae (92.16%). The improvement in histological, histochemical, and biochemical markers supported these findings.
Conclusion: Ivermectin loaded on solid lipid nanoparticles (SLNPS) could be an additional or synergistic therapeutic agent in treating trichinosis.
Keywords: Albendazole; Ivermectin; Muscular disease; Solid lipid nanoparticles; Trichinella spiralis.

INTRODUCTION

The nematode parasites from the genus *Trichinella* are the source of the food-borne helminthic infection known as trichinosis. *Trichinella spiralis*, or *T. spiralis*, is the most prevalent and harmful to humans. Intestinal symptoms are the first signs of trichinosis brought on by adults living in the small intestine. Larvae are then laid and move through the circulation. The most common manifestations of the parenteral phase are myalgia and periorbital edema. Finally, larvae settle and encyst in the active striated muscles of the host [1]. Trichinosis is commonly treated with traditional benzimidazoles like mebendazole and albendazole, although these drugs have limited absorption, no effect on the encapsulated larva, and are becoming increasingly resistant to treatment [2]. In addition, certain medications were shown to be carcinogenic [3]. Ivermectin (IVM) is a strong macrolytic lactone

that paralyzes worms and arthropods by allowing chloride ions to permeate the cell membrane [4]. In parasite nerve and muscle cells, it attaches itself to a glutamate-gated chloride channel receptor, thus impairing neurotransmission regulated by these channels. Loghry et al. (2020) examined the impact of IVM as an anti-filarial medication on extracellular vesicle secretion (EV). They also investigated motility and protein secretion and discovered that one characteristic of IVM that significantly inhibited nematode life stages and species (except for male parasites) was the inhibition of (EV) secretion. They deduced that part of the mechanism of action of IVM might be explained by inhibiting the secretion of (EVs). [5]. Although IVM effectiveness against trichinosis was reported, its effect was restricted to encysted muscle larvae [6]. This may be related to its poor water solubility, which results in reduced oral bioavailability. [7]. Therefore, improving IVM's effectiveness is essential, especially against encysted and migrating *T. spiralis* larvae [8]. The characteristic feature of nanomaterials is their dimension, which is less than 100 nanometers [9]. Nanotechnology's use in biological sciences aims to develop nano-carriers for sufficient and specific delivery of therapeutic agents [10]. Most employed NPs in drug delivery are liposomes and polymers [11]. Solid lipid nanoparticles, also known as SLNs, are a type of lipid nanoparticle that can serve as an alternate carrier for typical colloidal nanoparticles because of their diverse therapeutic uses. Drug distribution is greatly enhanced by liposomes, which are tiny solid particles suspended in a fluid phase [12]. The continuous release of a drug's contents and its stability at the nanoscale are essential for its effective delivery [13]. The purpose of our study was to evaluate the possible therapeutic impact of ivermectin-loaded solid lipid nanoparticles (IVM-SLNs) single or combined with albendazole against experimental muscular trichinosis.

METHODS

The study was conducted at Theodor Bilharz Research Institute (TBRI) in Giza, Egypt, during the period from May 2022 to May 2023.

Experimental animals and study groups: Seventy laboratory-bred parasite-free Swiss albino mice obtained from the animal house of TBRI, aging 5 weeks, weighing 20-25gm. Stool examination was done by direct smear and concentration techniques for 3 consecutive days to exclude any parasitic infections. Mice were divided into seven groups, 10 mice each. Group (I): negative control, group (II): infected, non-treated, group (III): infected and treated with albendazole, and group (IV): infected and treated with ivermectin. Group (V): infected and treated with solid lipid nanoparticles, group (VI): infected and treated with ivermectin loaded on solid lipid nanoparticles, and group (VII): infected and treated with a combination of albendazole and ivermectin loaded on solid lipid nanoparticles. Each group was subdivided into two subgroups (5 mice each) for the intestinal phase (7 days pi) and the muscular phase (49 days pi) that was included in our study. For parasitological, histopathological, and histochemical assessments, muscular specimens were collected from mice sacrificed on the 49th day PI.

The parasite and infection: The strain of Trichinella spiralis was isolated from infected mice in the animal house of Theodor Bilharz Research Institute (TBRI), Giza, Egypt. Sixty mice were infected orally with 200-250 larvae per mouse according to Wassom et al. [14].

Preparation of IVM-SLNs: By hot homogenization followed by ultrasonication method according to (Venkateswarlu &Manjunath,2004) [15]. The lipid phase consisted of IVM, lipid, and lipophilic surfactant; each weighed with an electronic balance (Shimadzu, Kyoto, Japan) and dissolved in a mixture of chloroform and methanol (2:1). The mixture was then transferred to a rota evaporator (IKA RV 10, Staufen, Germany) to remove organic solvents and obtain a thin lipid layer. Nitrogen was blown on the lipid layer to remove traces of vapors of organic solvents. The hot aqueous phase was heated to the same temperature as the molten lipid phase, added to the thin lipid layer, and hydrated for 30 min. Homogenization was carried out with the help of Ultra-turrax (IKA T 25, Staufen, Germany). The temperature was maintained at 5˚ C above the melting point of the lipid to prevent recrystallization. The obtained hot o/w emulsion was sonicated (13 mm probe) using UP200H ultrasonic homogenizer (Hielscher Ultrasonics GmbH, Teltow, Germany). The obtained hot nanoemulsion was quickly poured into 200 mL of cold water to get IVM-incorporated SLNs. The SLNs were collected by centrifugation at 15,000 g (Cooling Centrifuge, C-24 BL, REMI Ins. Ltd., Mumbai, India) for 90 min at 4˚ C and washed three times with purified water. The SLNs were suspended in purified water and kept under −40˚C

for 12 hrs. The samples were lyophilized for 48 h (Lyophilizer, Decibel, India) at - 40˚ C to remove water to keep them stable throughout storage. Mannitol (5% w/v) was used as a lyoprotectant. The obtained SLN powders were stored at 4˚ C. The control SLNs were prepared similarly without adding the IVM.

Characterization of nano-carriers: Scanning electron microscopy (SEM) was performed using SEM (SU1510 model; Hitachi Ltd., Tokyo, Japan) to study the morphological characteristics of prepared IVM-SLNs. Zeta sizer Nano Series (Malvern Instruments, UK) equipment was used to measure the zeta potential. Fourier transform infrared (FT-IR) (Thermo Scientific Nicolet 7199 FTIR spectrometer). Ultraviolet-visible (UV-VIS) spectra analysis (UV/VIS Spectrophotometer BK-UV1000G BK-V1000G).

Treatment Schedule & Dose: Ivermectin tablet (Iverzine 6mg ® UNI Pharma, Egypt) was given at a dose of 0.25 mg/kg body weight. on 35th days post-infection (dpi) single oral dose for the muscular phase [6]. Albendazole was available as Alzental suspension (EIPICO, Egypt), containing 20 mg/ml and given in a dose of 50 mg/kg orally for 7 successive days post-infection starting from 31st dpi for the muscular phase [16]**.** SLNPS suspension prepared by dissolving 5mg of SLNPS powder in 1ml of phosphate buffer saline (PBS) was administered in a single oral dose of 1.25mg/mouse [17] on 35th dpi for the muscular phase. Groups treated with ivermectin loaded on SLNPS and a combination of albendazole with ivermectin loaded on SLNPS were given the total dose of drugs on the same days.

Parasitological assessment:

For muscular encysted larval count, the entire diaphragm was dissected after scarification of mice on the (49th day PI), and then larvae were sedimented by centrifugation after digestion. The supernatant fluid was discarded and larvae in the sediment were counted using a McMaster counting slide to count the viable larva burden /mouse [18] according to this equation:

$$\frac{\text{Mean number of living larvae in both sides of the chamber}}{0.3}$$

Therapeutic effect assessment:

Drug efficacy (%) = [(A – B)/A] ×100, where A = the counted larvae of infected control mice, and B = the counted larvae from treated mice [19].

Histopathological assessment:

Mice were sacrificed on the 49th day post-infection (PI), and muscle specimens were taken from the diaphragm [20]. In 10% formalin, the specimens were fixed. dehydrated in increasing alcohol grades, cleared in xylol, implanted in paraffin blocks, sectioned at a thickness of 5 µ, stained with hematoxylin and eosin (H&E), and inspected under the microscope [3].

Histochemical study:

Feulgen stain was used to identify changes resulting from the hydrolysis of nuclear DNA acid due to apoptosis in the muscle tissues. Stained tissues were fixed avoiding strong acid application to prevent unnecessary de-staining. DNA stains bright red, and the background counterstains green. Apoptosis was classified according to changes in nuclear DNA coloration as light red, slight red, and less bright red representing extreme, moderate, and mild apoptosis, respectively. In contrast, bright red nuclei represent regular nuclei [21].

Biochemical assessment:

Blood samples were obtained from the retro-orbital vein of mice groups (II, III, IV, V, VI, and VII) using a disposable capillary tube at 30 dpi. Sera were isolated and utilized to assess the effect of drugs in treated mice groups on serum biochemical parameters, including liver parameters (total protein, albumin, globulin, AST & ALT), and renal parameters (urea, creatinine).

Ethical considerations:

Mice were maintained according to the research guidelines for the care and use of Laboratory Animals. Approval number: ZU-IACUC/3/F/91/2023.

STATISTICAL ANALYSIS

Data were analyzed by Statistical Package for Social Sciences (SPSS), windows version 20. Student (t) test and analysis of variance (ANOVA) test were performed for the probable differences among the studied groups. The P-value < 0.05 is considered significant. While <0.001 for highly significant results.

RESULTS

Characterization of SLNPS: Morphology analysis by SEM is shown in FS 1. The majority of particles were spherical and had smooth surfaces with a homogeneous polydispersity. The mean diameter obtained by SEM is smaller and ranges from 40 – 60 nm. The mean zeta potential of the synthesized NPs (FS 2) showed good stability with 52.3mV at 25.1°C with a conductivity of 0.127mS /cm. The mean particle size distribution of the NPs ranged from 20 – 60 nm the majority of particle size was 60 nm at 90° scattering angle under monodisperse form with total count ranging from 20000-640000

particles/ml. The Fourier transform infrared (FTIR) spectra of SLNP are presented in FS 3, the SLN nanoparticles spectrum represented by absorption peaks ranging from 350–1750 cm^{-1}. Five characteristic absorption peaks of SLNP are observed at 350, 650, 750, 900, 1560, and 1750 cm-1 representing the different main structures of SLNP. The Fourier transform infrared (FTIR) spectra of IVM loaded with SLN (SLNP-IVM) are presented in FS 4 that showed seven characteristic absorption peaks of SLNP-IVM at 150, 790,1200, 1550, 1760, 2000, and 2400 cm^{-}. FS 5 showed a characteristic single absorbance peak observed at 520nm showing the optical surface plasmon resonance (SPR) activity of the synthesized nano-particles. Loading IVM into the SLN nanoparticles caused characteristic absorbance peaks that were observed at 220 nm and 600 nm showing the optical surface plasmon resonance (SPR) activity of the synthesized nanoparticles loaded with IVM (FS 6).

Parasitological results:

Results of the muscular phase as shown in Tables (1,2) revealed that combined therapy (GVII) had the highest reduction in T.spiralis larvae number among the treated groups followed by GIII (albendazole alone) then GVI (treated with ivermectin loaded on solid lipid nanoparticles) with percentage reductions of 92.16%,90.11%, and 64.15% respectively with a high significant difference in between groups. The difference in larval count was significant among the studied groups except between control positive (GII) and (GV) treated with solid lipid nanoparticles. Insignificant differences also existed between GIII (treated with albendazole) and GVII (treated with a combination of albendazole and ivermectin loaded on solid lipid nanoparticles).

Histopathological results:

GI showed no histopathological changes (Fig. 1A). The control positive GII (Fig. 1B) muscle section showed infection by *T spiralis* intact encysted larva with no capsule surrounded by marked chronic lymphocytic infiltration. The muscle section of albendazole-treated mice (GIII) showed a shrunken *T. spiralis* encysted larva surrounded by mild chronic lymphocytic infiltration, one of the larvae is necrotic indicating moderate improvement (Fig. 1C). Muscle section of ivermectin-treated mice (GIV) showed multiple *T. spiralis* encysted larvae surrounded by moderate chronic lymphocytic infiltration (Fig. 1D). GV (Fig. 1E) treated with solid lipid nanoparticles showed massive infestation by T.spiralis larvae, surrounded by intense inflammatory reaction. The muscle section of GVI **(**infected and treated with SLNP +ivermectin**)** showed a moderate number of *T. spiralis* shrunken larvae surrounded by mild chronic lymphocytic infiltration (Fig. 1F). GVII that received mixed ivermectin loaded on solid nanoparticles and albendazole (Fig. 1G), showed normal muscle fibers with one T. spiralis larva which is necrotic and fibrosed and minimal inflammatory infiltration detected only by x400 power indicating best improvement.

Histochemical reactions:

GI (Fig. 2A) showed no histochemical changes while severe apoptosis was detected in GII (Fig. 2B) and GV (Fig. 2E). Moderate apoptosis was detected in GIV (Fig. 2D) and GVI (Fig. 2F). While G III (Fig.2C) and G VII showed mild apoptosis (Fig. 2G).

Biochemical results*:*

Biochemical study at 30dpi of all treated groups showed a highly significant decrease in serum activities of AST, ALT, urea, creatinine, and globulin when compared with their corresponding infected control group ($P<0.001$) (Table 3). A highly significant serum level elevation of the total protein and albumin ($P<0.001$) was noticed in all treated groups as compared with the corresponding infected control.

Table (1): The mean larval count of T. spiralis in the muscular phase in control and tested groups.

Group	Description	Larval count in the muscular phase		
		Mean ± SD	Range	R%
G II	Infected, non-treated (Positive control)	8925 ± 1100	7700 - 10200	
G III	Infected and treated with albendazole	882 ± 259	642 - 1246	90.11%
G IV	Infected and treated with ivermectin	4325 ± 350	3900 - 4700	51.54%
G V	Infected and treated with solid lipid nanoparticles	8600 ± 1309	7600 - 10500	3.64%

G VI	Infected and treated with ivermectin loaded on solid lipid nanoparticles	3200 ± 216	3000 - 3500	64.15%
G VII	Infected and treated with albendazole and ivermectin loaded on solid lipid nanoparticles	700 ± 183	500 - 900	92.16%
	F-test	98.666		
	P-value	<0.001**		

F: ANOVA test, **P:** Probability, **R%:** Reduction percentage ****:** Highly significant difference

Table (2): Least significant difference (LSD) test for comparison of mean number of T. spiralis encysted larva among control and other tested groups.

Post hoc test (LSD test) ***T.spiralis*** **larval count in the muscular phase**						
Groups	**G II**	**G III**	**G IV**	**G V**	**G VI**	**G VII**
G II						
G III	0.000**					
G IV	0.000**	0.000**				
G V	0.537	0.000**	0.000**			
G VI	0.000**	0.000**	0.043*	0.000**		
G VII	0.000**	0.728	0.000**	0.000**	0.000**	

Table (3): Comparison between the mean level of biochemical parameters in the muscular phase of T. spiralis in the control and tested groups.

Groups		**Total protein (g/dl)**	**Albumin (g/dl)**	**Globulin (g/dl)**	**Albumin/Globulin Ratio**	**AST (U/l)**	**ALT (U/l)**	**Creatinine (Mg/dl)**	**Urea (Mg/dl)**
G I	**Mean**	5.42	3.96	3.16	1.25	124.98	30.86	1.61	48.26
	S. D	0.17	0.17	0.17	0.01	15.11	2.44	0.18	4.75
G II	**Mean**	3.64	2.14	4.34	0.49	190.70	76.75	2.92	81.32
	S. D	0.50	0.05	0.25	0.02	9.47	5.93	0.18	3.99
G III	**Mean**	4.61	3.23	3.57	0.92	149.95	39.22	2.09	69.12
	S. D	0.29	0.10	0.39	0.14	4.47	3.46	0.39	7.06
G IV	**Mean**	4.01	2.87	3.90	0.74	173.30	57.51	2.54	74.72
	S. D	0.34	0.65	0.05	0.17	6.81	3.60	0.16	0.71
G V	**Mean**	3.75	2.65	4.00	0.66	177.29	68.51	2.73	76.72
	S. D	0.31	0.31	0.21	0.09	8.03	3.62	0.16	7.28
G VI	**Mean**	4.41	3.02	3.87	0.79	157.22	43.39	2.40	70.49
	S. D	0.21	0.37	0.65	0.12	16.49	0.97	0.06	6.50
G VII	**Mean**	5.10	3.53	3.41	1.04	142.72	32.67	1.92	54.60
	S. D	0.19	0.19	0.21	0.05	12.32	3.42	0.19	2.32
F-Test		24.42	16.86	7.15	30.34	20.38	123.37	24.52	26.95
P-value		<0.001**	<0.001**	<0.001**	0.944	<0.001**	<0.001**	<0.001**	<0.001**

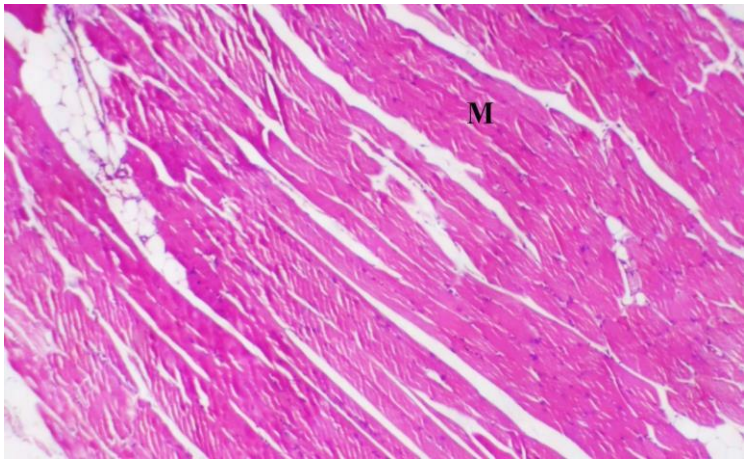

Figure (**1A**): Control-negative mice (GI) showed normal muscle fibers (M) with no parasitic infection and no inflammatory infiltration (H&Ex200).

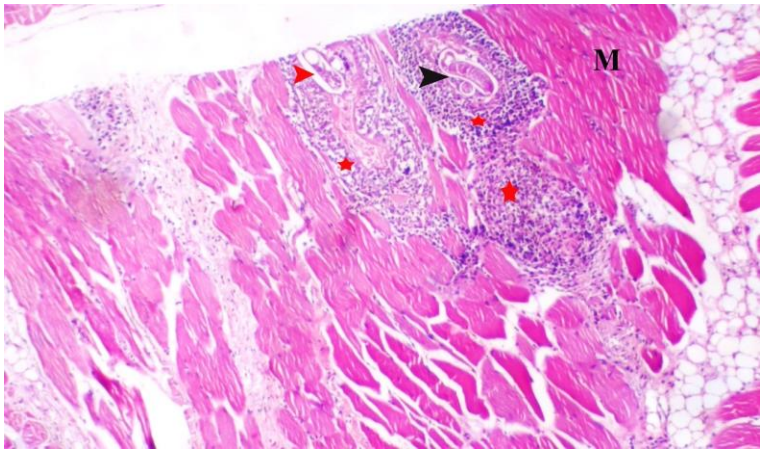

Figure(1B): Muscle section (M) of positive control (GII) showed infection by *T spiralis* intact encysted larva with no capsule (**arrowhead)** bisecting muscle layer and surrounded by marked chronic lymphocytic infiltration (**red star**) (H&Ex200).

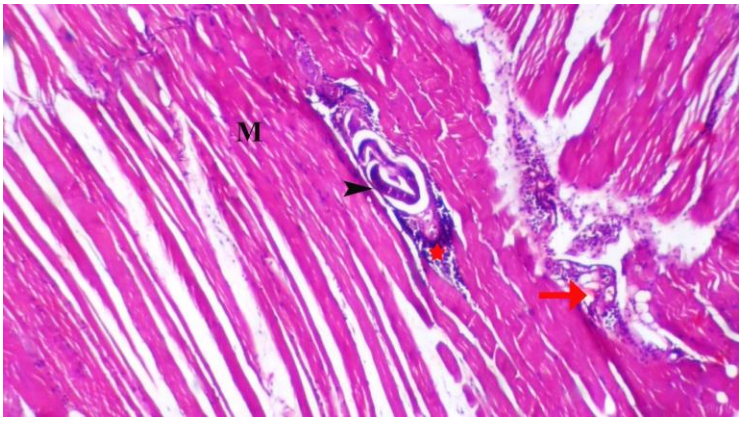

Figure (1C): The muscle section of albendazole-treated mice (GIII) showed shrunken *T. spiralis* encysted larva (**arrowheads**) bisecting muscle fibers (M) and surrounded by mild chronic lymphocytic infiltration (**red star**). One of the larvae is necrotic (**red arrow**) indicating moderate improvement (H&Ex200).

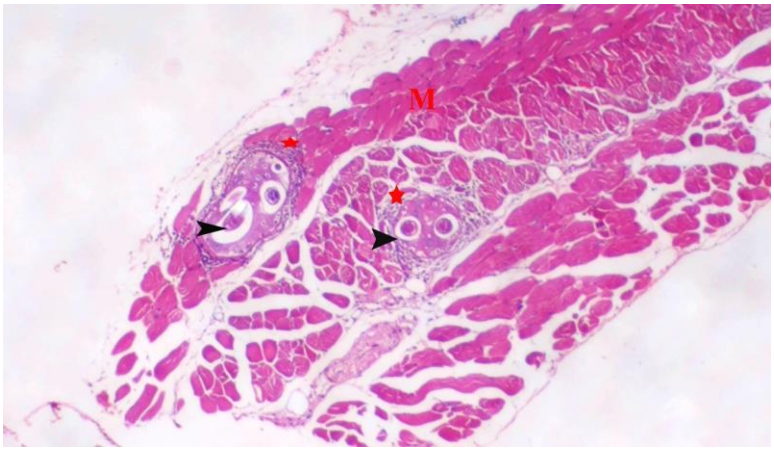

Figure (1D): Ivermectin-treated mice (GIV) showed a section in the muscle infected by multiple T. spiralis encysted larvae (**arrowheads)** bisecting muscle fibers (M) and surrounded by moderate chronic lymphocytic infiltration (**red star**). (H&Ex200).

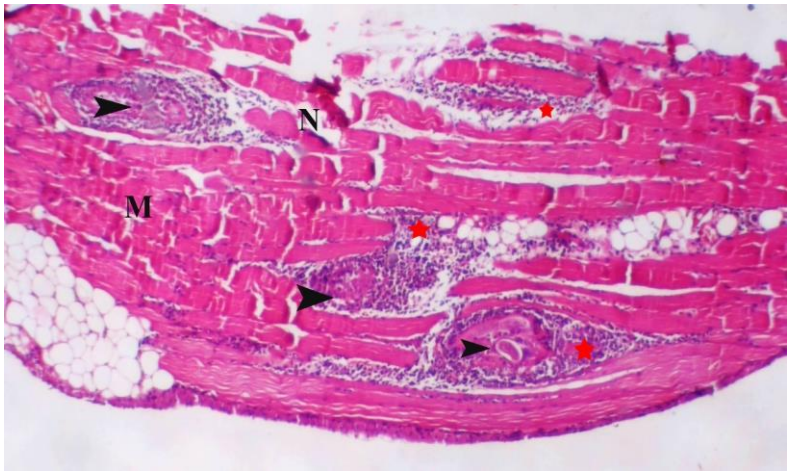

Figure (1E): Section in the muscle of GV (infected+ treated with SLNPS) infected by multiple *T. spiralis* encysted larvae (**arrowhead**) bisecting muscle fibers (M) and surrounded by marked chronic lymphocytic infiltration (**red star**) and areas of muscle necrosis (N). (H&Ex200).

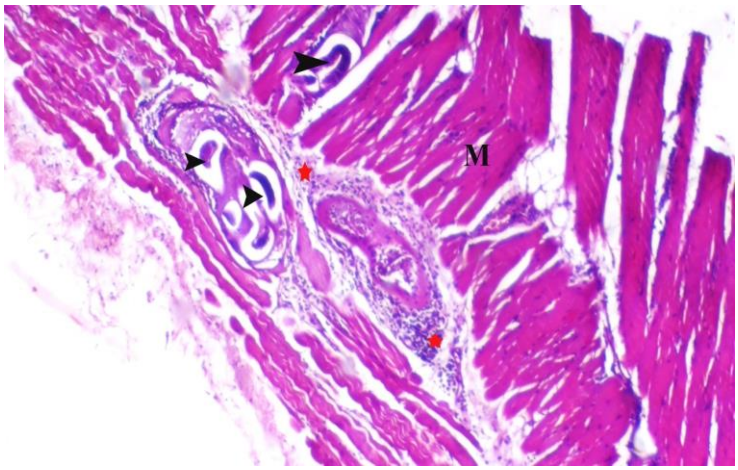

Figure (1F): Section in the muscle of GVI **(**infected treated with SLNP +ivermectin**)** showed a moderate number of T. spiralis shrunken larva (**arrowhead**) bisecting muscle fibers (M) and surrounded by mild chronic lymphocytic infiltration (**red star**). (H&Ex200).

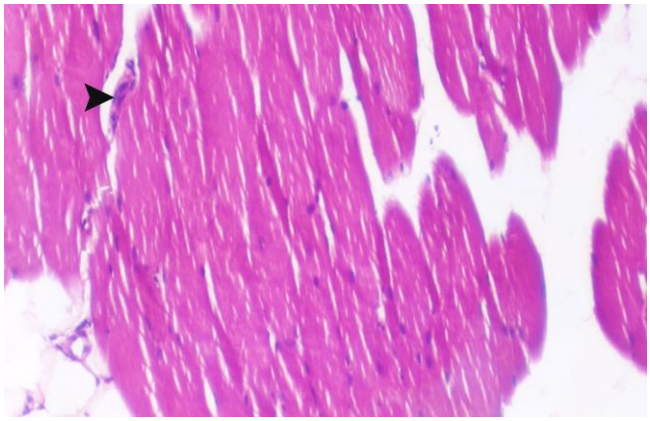

Figure (1G): GVII (infected and treated with ivermectin SLNPS +albendazole) showed normal muscle fibers with one T. spiralis larva (arrowhead) which is necrotic and fibrosed and minimal inflammatory infiltration indicating the best improvement (H&Ex200).

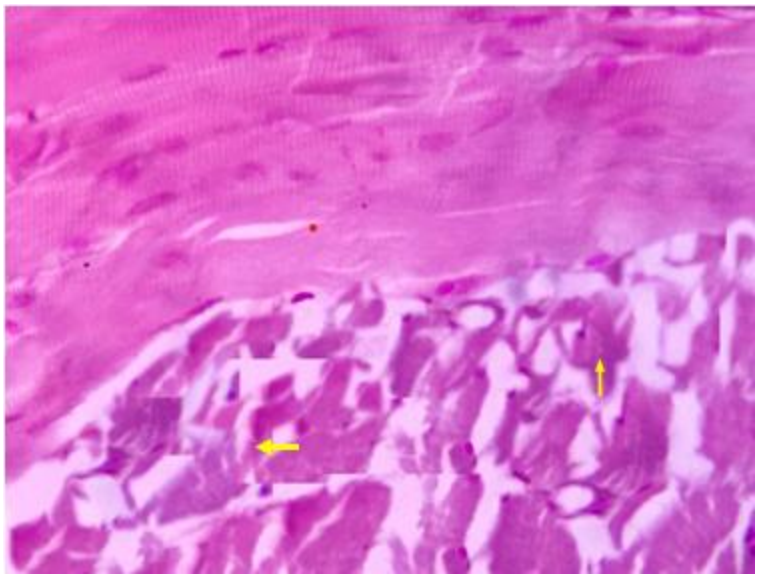

Figure (2A): Feulgen staining reaction of non-infected control mice (GI) showing normal muscular tissue (**yellow arrow)** X 100.

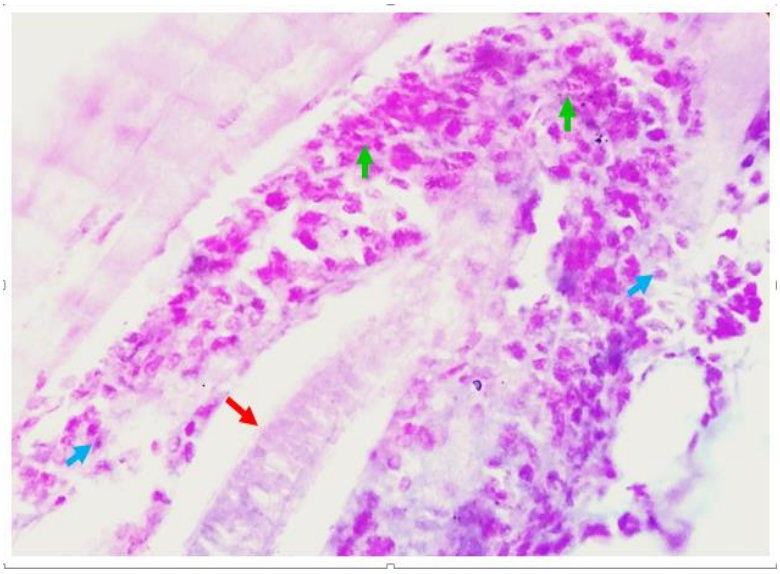

Figure (2B): Feulgen stain of control positive mice (GII) showing intact Trichinella larva (red arrow) surrounded by dense inflammatory reaction (green arrows) with the presence of a huge number of apoptotic cells with fragmented nuclei (light blue arrows) X 400.

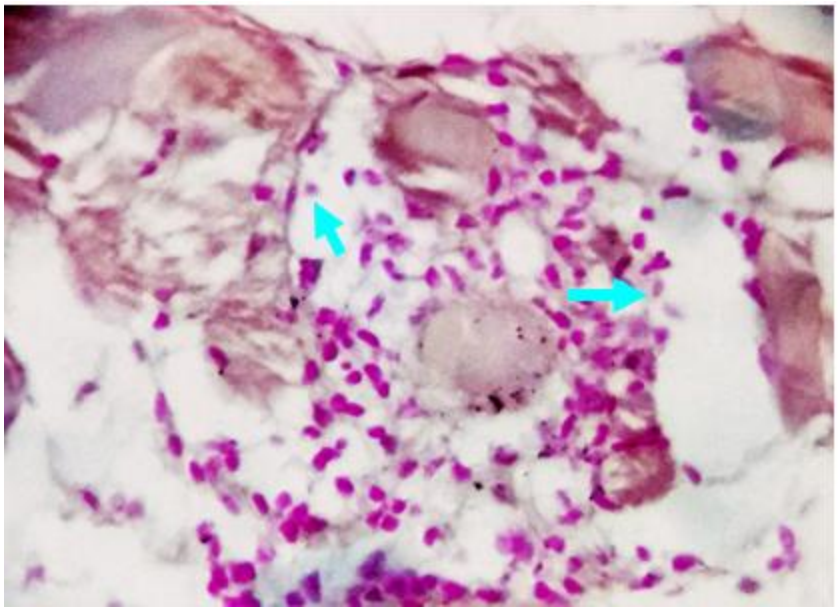

Figure (2C): Fuelgen stain of albendazole-treated mice (GIII) showing damaged Trichinella larva with the presence of mild inflammatory reaction including few apoptotic nuclei (light blue arrows). X 400.

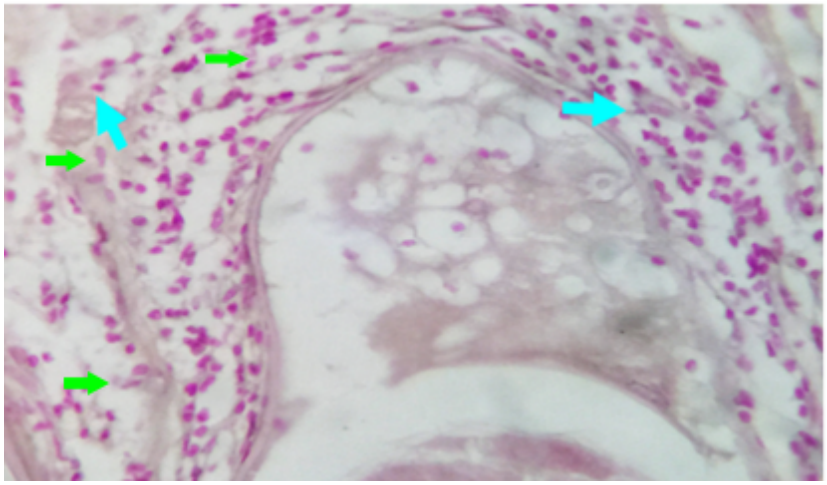

Figure (2D): Feulgen stain diaphragmatic muscle of ivermectin-treated mice (GIV) showing moderate inflammatory reaction with the presence of moderate apoptotic nuclei (light blue arrow) and fragmented nuclei (green arrow). X 400.

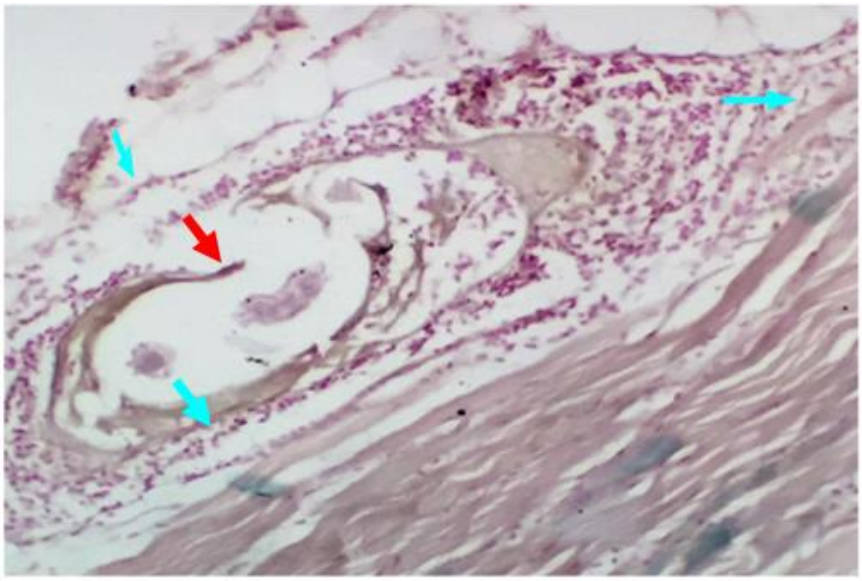

Figure (2E): Feulgen stain the diaphragmatic muscle of solid lipid nanoparticles treated mice (GV). Showing a nearly intact *Trichinella* larva, enclosed by a capsule (red arrow) surrounded by dense inflammatory reaction with the presence of many apoptotic cells (light blue arrows)**.** X 200.

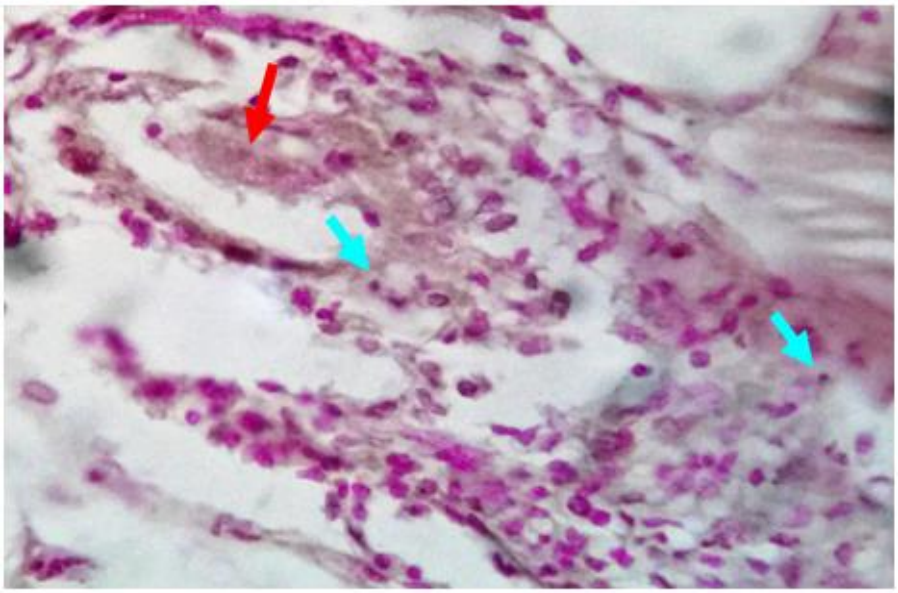

Figure (2F): Feulgen stain of the diaphragmatic muscle of GVI mice treated with ivermectin loaded on solid lipid nanoparticles showing partially destructed larvae of Trichinella (red arrows) with the presence of moderate inflammatory reaction including some apoptotic nuclei.(light blue arrows) X 400.

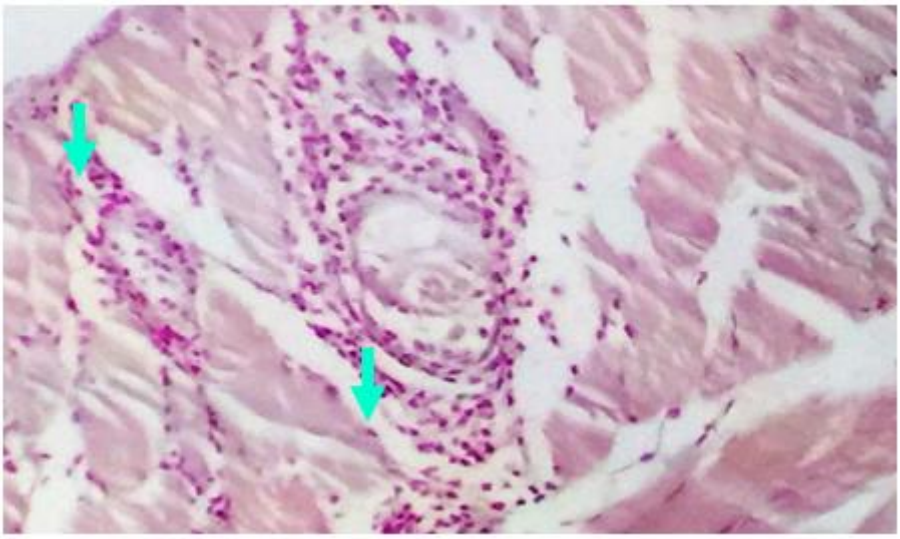

Figure (2G): Feulgen stain the diaphragmatic muscle of mixed ivermectin loaded on solid nanoparticles and albendazole-treated mice (GVII) showing destructed *Trichinella* larva surrounded by moderate inflammatory reaction including a few apoptotic nuclei. (Light blue arrows) .X 200.

DISCUSSION

The difficulty of treatment of T.spiralis infection is a leading cause for increasing the global burden of infection in addition to the limited bioavailability of specific drugs used for the treatment of trichinosis especially against the migrating and encysted larvae. Ivermectin is a broad-spectrum safe and tolerable antiparasitic drug but with low bioavailability after oral administration, because it is metabolized by the liver's cytochrome P450 system and it has a high affinity for plasma proteins (93.2 %) [22], this made the search for alternate methods for increasing the oral bioavailability of the drug and hence its therapeutic efficacy an urgent demand. SLNPs were offered as an alternative carrier to colloidal drug carriers [23]. The size of SLNs, are ranging from 50 to 1000 nm [24]. The large surface area, high drug loading properties, and higher stability enable the SLNPs to enhance the efficacy of the drugs [25]. The lipid matrix structure of solids (which is made of physiological lipids) reduces the toxicity of SLNPs and improves the absorption of water-insoluble drugs in the intestine [26].

The current study evaluated the therapeutic efficacy of ivermectin loaded on solid lipid nanoparticles with and without albendazole on experimental muscular trichinosis. The parasitological results revealed the highest reduction in the mean number of T.spiralis larval count was in GVII that received combination therapy of albendazole and ivermectin loaded on solid lipid nanoparticles, followed by GIII (treated with albendazole alone) with percentage reductions of 92.16% and 90.11% respectively. These results were similar to that recorded by Elmehy et al. (2021) [27] who tested the anti-trichinosis activity of a single oral dose of 200 µg/kg of niosomal IVM as compared to nano-crystalline form on both adult and larval counts when administered on 1st, 10th, and 30th dpi, respectively. This also agreed with Soliman et al. (2011) [6] as they showed that a single subcutaneous dose of 0.2mg/kg IVM at 10th dpi reduced the larvae in diaphragms of infected rats, while unsuccessful in reduction of larval counts occurred when injected at 35 dpi because it cannot cross the capsule of the nurse-cell complex and kill the parasites inside. Basyoni and El-Sabaa (2013) [28] tested IVM administration on 0 and 5 dpi and reported high efficacy of IVM in killing adult T. spiralis (98.5% and 80%) respectively, while drug efficacy against encysted muscle larvae decreased as the treatment given 15 dpi and 35 dpi (76.5% and 54%). The mechanism of action of IVM depends on interference with the nervous system and muscle functions by improving inhibitory neurotransmission [29]. Ivermectin paralyzes worms and arthropods by allowing chloride ions to permeate the cell membrane [4] by binding to a glutamate-gated chloride channel receptor in parasite nerve and muscle cells resulting in impairing neurotransmission regulated by these channels. The ability of ivermectin loaded on solid lipid nanoparticles to attack the adults and the larvae with high efficacy can be explained by the enhanced oral bioavailability that solid lipid nanoparticles induce with the resulting increase in drug plasma concentration. Lipid nano-carrier showed similar

results regarding drug enhancing effect with Ibrahim et al. (2024) [30]. They assessed the effect of chitosan-coated lipid nano-combination with albendazole and miltefosine (MFS) in treating experimental murine trichinosis and found that the most effective drug was nanostructured lipid carriers (NLCs) loaded with ABZ which showed the most significant reduction in adults and larval count (100% and 92.39%, respectively).

In the present study, the histopathological findings in diaphragmatic muscle sections from the positive control mice (GII) showed massive infestation by Trichinella spiralis larvae surrounded by intense inflammatory reaction. These findings agreed with [31] and [32]. Trichinella spiralis larvae produce high levels of oxygen-reactive species that induce inflammation in addition to mechanical damage to myocytes. After that, a collagen capsule is formed to support the larvae inside its muscle niche for a long time and is the cause of decreased efficacy trichinosis trichinosis-specific drugs against the encysted larvae [33]. In the present study, the muscle tissue of all treated mice groups showed fewer T.spiralis larvae, most of them are destructed and surrounded by a thin destructed capsule and mild inflammatory reaction. Marked improvement was noticed in the group treated with the combination of ivermectin loaded on solid nanoparticles and albendazole (GVII). The present findings were supported by those recorded by Basyoni and El-Sabaa (2013) [28] who noticed that muscular tissue degenerative alterations decreased while fragmentation of larva was augmented on administration of IVM 15 dpi compared to less t effects induced by IVM 35 dpi because of their low water solubility that limits its absorption. [34] also supported the current results, they revealed a decrease in the amount of collagen fibers around encysted larvae in muscles of mice treated with mebendazole-loaded silver nanoparticles. Our results agreed also that obtained by [27] and they concluded that niosomal IVM could be an effective new therapy for trichinellosis.

Apoptosis is a method for programmed cell death that controls cell proliferation [35]. Parasites might induce apoptosis directly through active mediators or indirectly through inflammatory mediators [36].

Our histochemical results in the muscle phase revealed severe apoptosis in the positive control GII and GV that received only solid lipid nanoparticles. Moderate apoptosis was observed in groups receiving treatment with ivermectin single and loaded on SLNP (GIV and GVI). Meanwhile, G III and G VII, treated with albendazole single and combined with IVM loaded on SLNPs, showed mild apoptosis. These results were consistent with [32] (Sarhan et al. 2021), who noted marked apoptosis in the muscle tissue of the positive control group, which displayed nuclear disintegration and a light red coloring of the muscle cell nuclei next to the larvae. In addition, Etewa et al. 2018 [37] reported marked apoptosis in experimental trichinosis in the positive control group, demonstrating the parasite's destructive effect on the muscle cells. Apoptosis associated with experimental trichinosis was reported by [38]. They added that apoptotic cells in the inflammatory infiltration were noted much more frequently in the muscular phase than in the small intestine's lamina propria. Muscle cell necrosis happens when there is significant damage. Because of this damage, cells cannot be repaired, and scavenger cells eliminate the necrotic region by phagocytosis. Apoptosis is a process that muscle cells might go through, or they can self-repair after being exposed to little damage. [39]. Matsuo et al. (2000) [40] reported different features of basophilic cytoplasm in muscle cells which are characteristic of apoptosis.

Concerning the biochemical assessment, all treated mice groups showed an increase in total proteins and a significant decrease in AST and ALT, urea, and creatinine levels with a highly significant difference compared to the positive control group. Soliman et al. (2011) reported similar results [6] after treatment of T.spiralis - infected rats with a single dose of ivermectin 0.2mg/kg S.C. on the 4th dpi. They attributed the results to drug larvicidal activity. Basyoni and El-Sabah (2013) [28] investigated the possibility of using ivermectin and myrrh as treatments for experimental trichinosis and they found similar biochemical results. This also agreed with Nada et al. (2018) [31], who reported reductions in the levels of urea, creatinine, AST, ALT, and CPK but a rise in total proteins in mice treated with Nigella sativa, ivermectin versus albendazole compared to the infected non-treated group.

The present study's findings demonstrated that ivermectin loaded on solid lipid nanoparticles achieved better results during the treatment of muscular trichinellosis especially when combined with albendazole.

CONCLUSIONS

Our study results suggest that ivermectin loaded on solid lipid nanoparticles alone or combined with albendazole could be used with high efficacy as a synergetic or new therapeutic agent against trichinosis infection. Further research is needed with

trials of different doses, routes of administration, and different nanocarriers. Testing the effect of ivermectin on certain parasite targets like parasite extracellular vesicles may be searched.

Conflict of Interest: None.
Funding Statement: None.

REFERENCES

1.Taher E, Meabed E, El Akkad D, Kamel N and Sabry M. Modified dot-ELISA for diagnosis of human trichinellosis. Exp Parasitol 2017; 177: 40-46. https://doi.org/10.1016/j.exppara.2017.04.002.

2. Prichard R. Markers for benzimidazole resistance in human parasitic nematodes, Parasitol 2007; 134 (8): 1087–92. https://doi.org/10.1017/S003118200700008X.

3. Shalaby M, Moghazy F, Shalaby H, Nasr S. Effect of methanolic extract of Balanites aegyptiaca fruits on enteral and parenteral stages of *Trichinella spiralis* in rats. Parasitol Res 2010; 107:17-25. https://doi.org/10.1007/s00436-010-1827-9.

4. **Chippaux J, Boussinesg M and Prod'hon J.** The use of ivermectin in control of onchocerciasis. Sante 1995; 199(5):149–58.

5. **Loghry H, Yuan W, Zamanian M, Wheeler N, Day T, Kimber M**. Ivermectin inhibits extracellular vesicle secretion from parasitic nematodes. *J. Extracell.Vesicles* 2020; 10: e12036. https://doi.org/10.1002/jev2.12036

6. **Soliman G, Taher E. and Mahmoud M.**: Therapeutic efficacy of dormectin, ivermectin and levamisole against different stages of *Trichinella spiralis* in rats. Türkiye Parazitolojii Dergisi, 2011; 35(2):86–91.

7. Lu M, Xiong D, Sun W, Yu T, Hu Z, Ding J, et al. Sustained release ivermectin-loaded solid lipid dispersion for subcutaneous delivery: in vitro and in vivo evaluation. Drug Deliv 2017**;** 24(1): 622–31. https://doi.org/10.1080/10717544.2017.1284945.

8. Bai X, Hu X, Liu X, Tang B, Liu M. Current research of trichinellosis in China. Front Microbiol 2017; 8:1472. https://doi.org/10.3389/fmicb.2017.01472.

9. Jeevanandam J, Barhoum A, Chan Y, Dufresne A, Danquah M. Review on nanoparticles and nanostructured materials: history, sources, toxicity and regulations. Beilstein J Nanotechnol 2018; 9:1050–74. https://doi.org/10.3762/bjnano.9.98.

10. Havel H, Finch G, Strode P, Wolfgang M, Zale S, Bobe I, et al. Nanomedicines: from bench to bedside and beyond. AAPS J 2016; 18(6):1373–8. https://doi.org/10.1208/s12248-016-9961-7.

11. Ventola C. Progress in nanomedicine: approved and investigational nanodrugs. Peer-Rev J Formul Manag 2017; 42(12):742–55.

12. Weers J. Colloidal particles in drug delivery. Curr Opin Colloid Interf Sci. 1998; 3(5):540–4. https://doi.org/10.1016/S1359-0294 (98) 80030-7.

13. Nagati V, Tenugu S, Pasupulati A. Chapter 4-Stability of therapeutic nano-drugs during storage and transportation as well as after ingestion in the human body. In: Das Talukdar A, Dey Sarker S, Patra JK, editors. Advances in nanotechnology-based drug delivery systems. Amsterdam: Elsevier; 2022; 83–102. https://doi.org/10.1016/B978-0-323-88450-1.00020-X.

14. **Wassom D, Wakelin D, Brooks B, Krco C, David C.** Genetic control of immunity to *Trichinella spiralis* infections of mice. Hypothesis to explain the role of H-2 genes in primary and challenge infections. Immunol 1984; 51(4):625-31. PMID: 6423524; PMCID: PMC1454539.

15. **Venkateswarlu V, Manjunath K.** Preparation, characterization and in vitro release kinetics of clozapine solid lipid nanoparticles. J Control Release 2004; 95(3):627-38. https://doi: 10.1016/j.jconrel.2004.01.005. PMID: 15023472.

16. Attia R, El-sayed M, Farrag H et al. Effect of myrrh and thyme on *Trichinella spiralis* enteral and parenteral phases with inducible nitric oxide expression in mice. Memórias do Instituto Oswaldo Cruz 2015; 110 (8): 1035-41. https://doi.org/10.1590/0074-02760150295.

17. Hassan M, El-Rahman A, Mostafa E, El-Hamed A, Fakhry E, Abdel Fattah A, et al. The impact of nitazoxanide loaded on solid lipid nanoparticles on experimental trichinellosis**.** ZUMJ 2021; 27(6):1074-84. https:// doi: 10.21608/zumj.2019.16531.1480.

18. Dunn I J, Wright K A. Cell injury caused by Trichinella spiralis in the mucosal epithelium of B10A mice. J Parasitol 1985; 71(6):757-66. https://doi.org/10.2307/3281709.

19. Hosking B, Watson T, Leathwick D. Multigeneric resistance to oxfendazole by nematodes in cattle. Vet Rec 1996; 138(3):67-8. https://doi: 10.1136/vr.138.3.67.

20. Monib M, Shaheen M, Galal L, Farrag H. Role of T.spiralis adult and larval antigens in immunomodulation of nitric oxide (NO) in intestinal and muscular phase of trichinelosis. Assiut Med J 2010; 34:147-58.

21. Chieco P, Derenzini M. The Feulgen reaction 75 years on. Histochem Cell Biol 1999; 111(5):345-58. https://doi.org/10.1007/s004180050367.

22. De Castro G, Gregianin L, Burger J. Continuous high dose ivermectin appears to be safe in patients with acute myelogenous leukemia and could inform clinical repurposing for COVID-19 infection. Leuk Lymphoma 2020**;** 61(10): 2536-37. https://doi.org/10.1080/10428194.2020.1786559.

23. Allen T, Cullis P. Liposomal drug delivery systems: from concept to clinical applications. Adv Drug Deliv Rev 2013; 65(1):36–48. https://doi.org/10.1016/j.addr.2012.09.037.

24. Nicolas J, Mura S, Brambilla D, Mackiewicz N, Couvreur P. Design, functionalization strategies and biomedical applications of targeted biodegradable/biocompatible polymer-based nanocarriers for drug delivery. Chem Soc Rev 2013; 42(3):1147–235. https://doi.org/10. 1039/c2cs35265f.

25. Jacob S, Nair A, Shah J, Gupta S, Boddu S, Sreeharsha N, et al. Lipid nanoparticles as a promising drug delivery carrier for topical ocular therapy-an overview on recent advances. Pharm 2022; https://doi.org/10.3390/pharmaceutics14 030533.

26. Satapathy S, Patro C. Solid lipid nanoparticles for efficient oral delivery of tyrosine kinase inhibitors: a nano targeted cancer drug delivery. Adv Pharmaceut Bull 2022;12(2):298–308. https://doi.org/10.34172/apb.2022.041.

27. Elmehy D, Hasby M, El Maghraby G, Arafa M, Soliman N, Elkaliny H, et al. Niosomal versus nano-crystalline ivermectin against different stages of Trichinella spiralis infection in mice. Parasitol Res 2021; 120(7):2641-58. https:// doi: 10.1007/s00436-021-07172-1. Epub 2021 May 4. PMID: 33945012.

28. Basyoni M, El-Sabaa A. Therapeutic potential of myrrh and ivermectin against experimental *Trichinella spiralis* infection in mice. Korean J Parasitol 2013; 51(3):297–304. https://doi.org/10.3347%2Fkjp.2013.51.3.297.

29. Yates D, Wolstenholme A. An ivermectin-sensitive glutamategated chloride channel subunit from Dirofilaria immitis. Int J Parasitol 2004; 34 (9):1075–81.
https://doi.org/10.1016/j.ijpara.2004.04.010.

30. Ibrahim A, Selim S, Shafey D, Sweed D, Farag S, Gouda M. Appraisal of Chitosan-Coated Lipid Nano-Combination with Miltefosine and Albendazole in the Treatment of Murine Trichinellosis: Experimental Study with Evaluation of Immunological and Immunohistochemical Parameters. Acta Parasitol 2024;1-22. https://doi.org/10.1007/s11686-024-00799-x.

31. Nada S, Mohammad S, Moad H, El-Shafey M, Al-Ghandour A, & Ibrahim N. Therapeutic Effect of Nigella Sativa and Ivermectin versus Albendazole on Experimental Trichinellosis in Mice. J Egypt Soc Parasitol 2018**;** 48(1): 85-92. https://doi.org/10.21608/jesp.2018.77029.

32. Sarhan M, Etewa S, Al-Hoot A, Arafa S, Shokir R, Moawad H, et al. Stem cells as a potential therapeutic trend for experimental trichinosis. Parasitol United J 2021; 14(2):151-61.

33. **Bruschi F, Chiumiento L**. Trichinella inflammatory myopathy: host or parasite strategy? Parasit Vectors 2011; 4 (1):42. http://www.parasitesandvectors.com/content/4/1/42.

34. **El-Melegy M, Ghoneim N, El-Dienos N and Rizk M.** Silver nano particles improve the therapeutic effect of mebendazole treatment during the muscular phase of experimental trichinellosis. J Am Sci 2019; 15(5). http://www.jofamericanscience.org/

35. Osborne B. Apoptosis and the maintenance of homoeostasis in the immune system. Curr Opin Immunol 1996; 8(2):245-54. https://doi.org/10.1016/S0952-7915(96)80063-X.

36. Lundy S, Lerman S and Boros D. Soluble egg antigen stimulated T helper lymphocyte apoptosis and evidence for cell death mediated by FasL(+) T and B cells during murine Schistosoma mansoni infection. Infect Immun 2001; 69(1):271-80. https://doi.org/10.1128/iai.69.1.271-280.2001.

37. Etewa S, Fathy G, Abdel-Rahman S, El-Khalik D, Sarhan M, Badawey M. The impact of anthelminthic therapeutics on serological and tissues apoptotic changes induced by experimental trichinosis. J Parasit Dis 2018; 42(2):232-42. https://doi.org/10.1007/s12639-018-0990-2.

38. Karmańska K, Houszka M, Piekarska J. The phenomenon of apoptosis in the course of experimental trichinellosis in mice. Wiad Parazytol 2000; 46(1):111-15.

39. Wu Z, Nagano I, Takahashi Y. Candidate genes responsible for common and different pathology of infected muscle tissues between *Trichinella spiralis* and T. pseudospira-lis infection. Parasitol Int 2008**;** 57:368-78.
https://doi.org/10.1016/j.parint.2008.03.005.

40. **Matsuo A, Wu Z, Nagano I, Takahashi Y.** Five types of nuclei present in the capsule of Trichinella spiralis. Parasitol 2000**;** 121:203-10. https://doi.org/10.1017/S0031182099006198.

SUPPLEMENTARY FIGURES

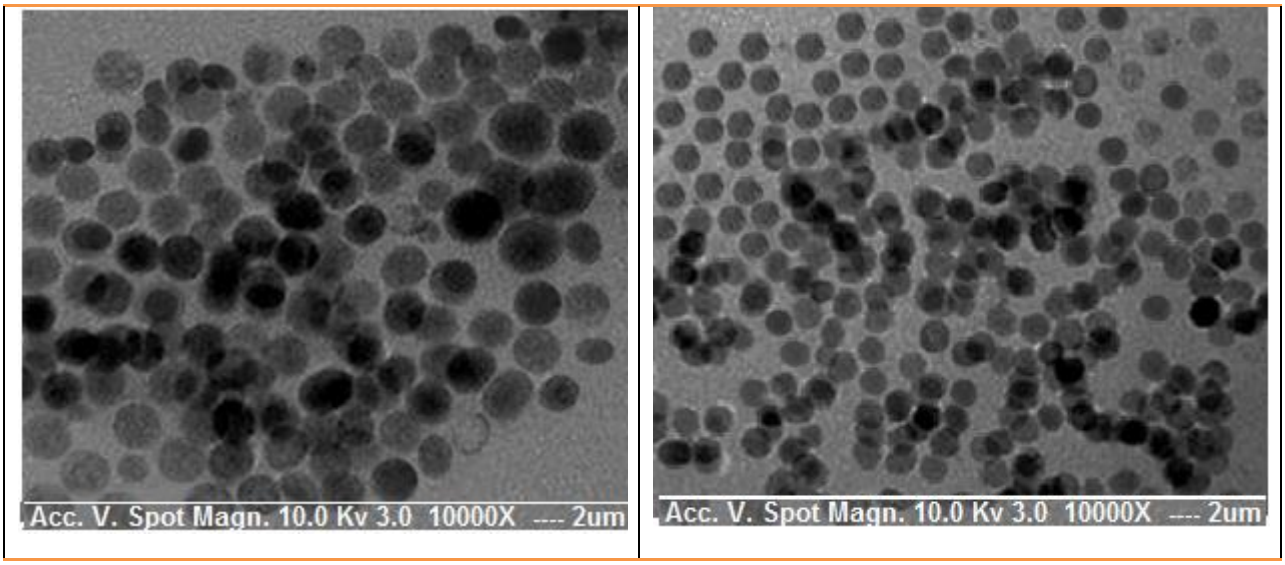

FS 1: SLN morphology analysis by SEM, the majority of particles were spherical and had smooth surface with a homogeneous polydispersity. The mean diameter obtained by SEM is smaller and ranged from 40 – 60 nm.

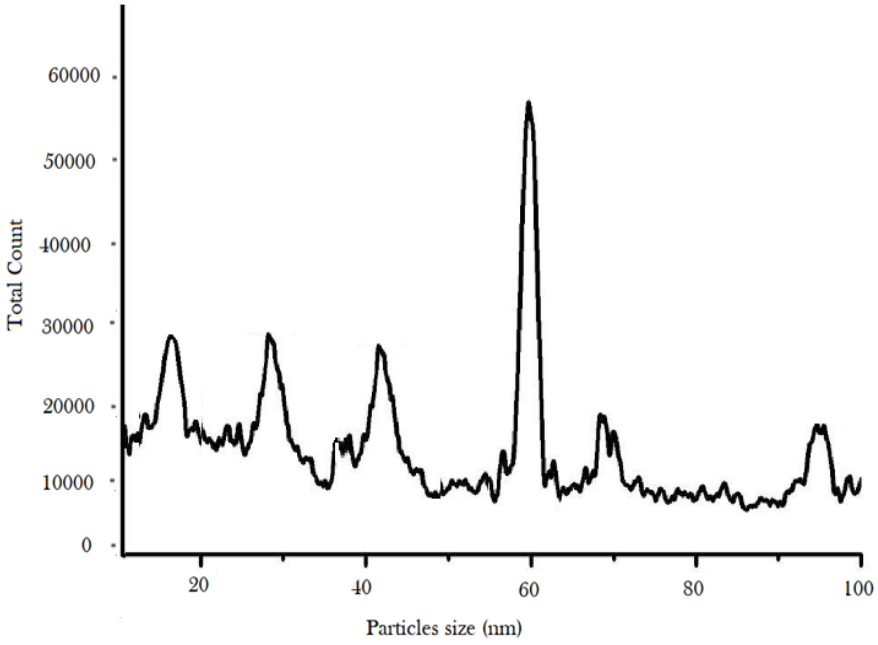

FS 2: The mean zeta potential of the synthesized NPs.

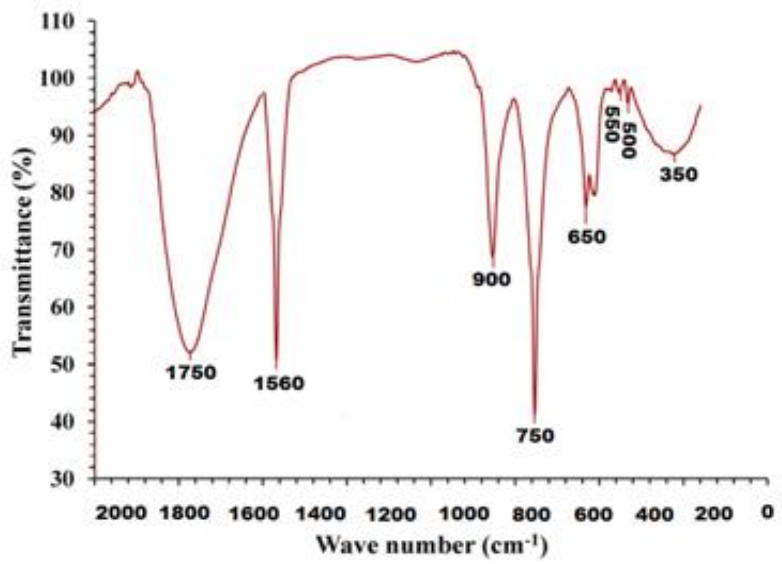

FT-IR analysis.

FS 3: FTIR spectra of SLN (SLNP) Five characteristic absorption peaks of SLNP are observed at 350, 650, 750, 900, 1560, and 1750 cm^{-1} representing the different main structure of SLNP.

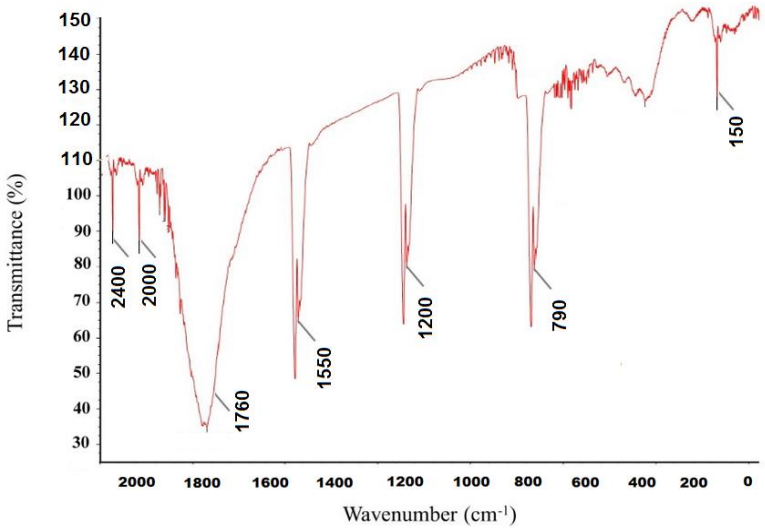

FS 4: The Fourier transform infra-red (FTIR) spectra of IVM loaded with SLN (SLNP-IVM) **Seven** characteristic absorption peaks of SLNP-IVM are observed at 150, 790 , 1200, 1550, 1760, 2000 and 2400 cm^{-1} .

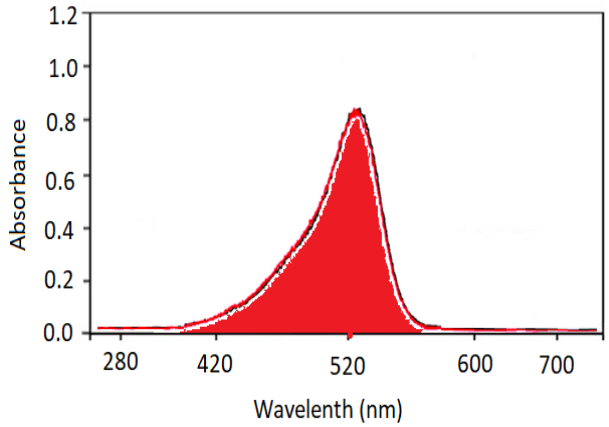

FS 5: A characteristic single absorbance peak observed at 520nm showing the optical surface plasmon resonance (SPR) activity of the synthesized nanoparticles.

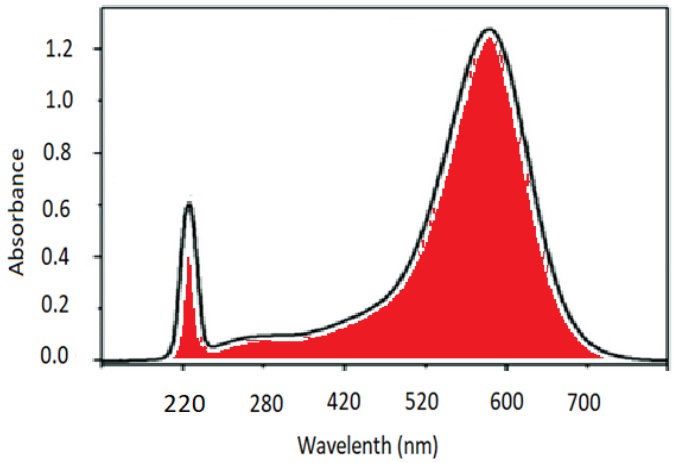

FS 6: A characteristic absorbance peaks was observed at 220nm and 600 nm showing the optical surface plasmon resonance (SPR) activity of the synthesized nanoparticles loaded with IVM .

To cite:

Farag, T., Almotayam, M., Mohamed, A., Al-Attar, A. R., Aly, I., Farag, S., Hammad, S. Assessment of the Therapeutic Impact of Ivermectin Loaded on Solid Lipid Nanoparticles against Muscular Phase of Murine Trichinosis. *Zagazig University Medical Journal*, 2024; (1449-1465): -. doi: 10.21608/zumj.2024.279448.3283